



## ENHANCEMENT THE HEAT TRANSFER FOR TWO-PHASE FLOW THROUGH A RECTANGULAR RIBBED VERTICAL CHANNEL

Riyadh S. Al-Turaihi      Doaa Fadhil kareem  
drriyadhalturaihi@yahoo.com      yg77597@gmail.com  
Mech. Eng. Department, University of Babylon, Hilla, Iraq

### ABSTRACT

The heat transfer coefficient and temperature distribution of two phase flow (water, air) in rectangular ribbed vertical channel was investigated experimentally and numerically in this work for different values of water and air superficial velocities (0.0421, 0.0842, 0.1158, 0.1474 and 0.1684 m/s) and (1.0964, 1.425, 1.644, 1.864 and 2.193 m/s), respectively, at constant heat flux (120 W). The distribution of temperature along the channel was photographed using thermal camera and compared with images for the corresponding contours which found numerically. The experimental results of heat transfer coefficient compared with computational fluid dynamics model simulated by Ansys fluent 15.0. A good agreement has been found between the experimental and numerical data, where the percentage deviation between the experimental and the numerical results is (1% - 6%). The results showed that, the local heat transfer coefficient increased by adding ribs, it also increased as the velocity of the flow increased.

**KEY WORDS :** two-phase flow, Heat transfer, ribbed channel, turbulent flow , CFD, Ansys Fluent .

### تحسين انتقال الحرارة لجريان ثنائي الطور خلال قناة مستطيلة عمودية مضلعة

دعاء فاضل كريم

رياض صباح صالح الطريحي

#### الخلاصة:

يتضمن هذا العمل دراسة عملية و نظرية لتوزيع معامل انتقال الحرارة ودرجات الحرارة لجريان ثنائي الطور (ماء - هواء) في قناة عمودية مضلعة مستطيلة لقيم سرعة متعددة للماء و الهواء عند فيض حراري ثابت (120 واط). تم تصوير توزيع درجة الحرارة على طول القناة باستخدام كاميرا حرارية وتم مقارنتها مع النتائج النظرية. تمت مقارنة النتائج العملية لمعامل انتقال الحرارة مع النتائج النظرية باستخدام برنامج (انسز-فلونت نسخة 15.0). تم ايجاد توافق جيد بين النتائج العملية والنظرية لمعامل انتقال الحرارة مع نسبة تفاوت تتراوح بين (1-6%). اظهرت النتائج ان معامل انتقال الحرارة يزداد عند اضافة العوائق، وكذلك يزداد عند زيادة سرعة الجريان.

## INTRODUCTION

Different methods have been developed to improve the rate of heat transfer, and they are characterized as either passive or active technique. Passive techniques include additives of fluid, devices of swirl flow, extended and coated surfaces, and roughed surfaces anything that include applying special surface geometry. While active techniques include vibration of surface, acoustic or electric fields, and mechanical aids simply the techniques that requisite external power source (**Manca et al. 2011**). Channels and pipes that roughed with ribs or grooves are widely used in several applications such as ventilation, turbine blades, heat exchangers, and refrigeration. This is because of their desirable characteristics such as high heat and mass transfer rates between phases, temperature homogeneity, and good mixing of phases. One of the successful techniques is the use of ribs or grooves in the channels. The design of the ribs depends on its application. Ribbed channels are commonly used for the improvement of convection heat transfer. Since the presence of ribs in the channels generated a turbulence flow by breaking the laminar sub - layer if compared with the smooth channel, and this leads to increase the rate of heat transfer. Also the thermal boundary layer thickness are reduced by ribs due to the secondary flow regions that appear near the wall which increase the heat transfer rate. This work can be accomplished by maintaining the height of the roughness parts small compared with the dimensions of the channel (**Ansari and Arzandi, 2012**). Several researcher studied the ribbed channels, **Vlasogiannis et al. (2002)**, experimentally measured the local heat transfer coefficient for flow of water and air in a plate heat exchanger, **Shedd and Newell (2003)**, proposed throughout experimental explanations of the liquid film thickness profiles of adiabatic two phase flow (water-air) in a lucid pipes with 20 microgrooves located at three various helix angles ( $0^\circ$  (axial),  $9^\circ$ , and  $18^\circ$ ), **Asano et al. (2004)**, experimentally studied the adiabatic two phase flow (water-air) and R141b boiling two phase flow in heat exchangers with a single channel located vertically, **Jayakumar et al. (2010)**, theoretically studied the thermal hydraulics of two-phase flow in a helically coiled heat exchanger using CFD, Fluent 6.3 modeling multiphase flow Euler-Euler model. The effects of the pitch coil, diameter of the pipe, and pitch circle diameter on the patterns of the flow in a helical pipes were investigated, **Wang et al. (2010)**, theoretically formed a model to simulate the three - dimensional flow with heat transfer of air and steam in a serpentine cooling channels using CFX approach. The flow in smooth and ribbed channels was described by using the SST and SSG turbulence model, respectively, **Ansari and Arzandi (2012)**, experimentally investigated the air water two phase flow using rectangular ducts that are smooth and ribbed to show the effect of ribs height on the boundaries, they also presented a flow map diagram, **Saha and Saha (2013)**, determined the experimental Nusselt number and friction factor data of laminar flow in a circular channel had an integral helical rib roughness and fitted with wavy-tape inserts, **Al-Turaihi and Olewi (2016)**, employed a CFD model to study the two-phase flow in smooth and ribbed channels. Temperature was applied for the top and the bottom of the channel where the ribs located. Three kinds of ribs were used to perform the experiments triangle, rectangular, and trapezoidal, **Jalghaf et al. (2016)**, investigated experimentally and numerically the two phase unsteady flow around heated body (circular-cylinder) in a horizontal rectangular channel. In this work a computational fluid dynamics simulation was performed for a two phase (water-air) flow in ribbed and smooth channel. Three rib shapes was used (triangular, semi-circle, and rectangular) and the results are compared with smooth channel to show the effect of ribs on the heat transfer coefficient.

## EXPERIMENTAL TEST

An experimental channel is constructed to study the effect of water and air superficial velocities, also to show the effect of the ribs shape on the temperature distribution and heat transfer coefficient. The equipment used for the experimental test and the measuring system is shown in figure (1). Perspex transparent channel used with a rectangular cross section (10 cm × 3 cm) and a length (70 cm) with a water pipe has a diameter of (3.175 cm), and air pipe has a diameter of (1.27 cm) to report the demeanor of the mixture (water – air) over the heated plate (rib). Channel has five holes at different locations, and sensors are fixed to measure the temperature of the two-phase flow inside the channel. Ribs are design and manufactured from stainless steel material with thermal conductivity of (202.4 W/m. k). Three different shapes of ribs was studied which as (triangular, semi-circle, and rectangular) as shown in figure (2), smooth channel was also generated to show the difference made by the ribs. The ribs have a base width of ( $p=1.2$  cm) and height of ( $d=0.6$  cm) along with a pitch distance of ( $w=0.5$  cm). Ribs are mounted and fixed by screw and nut on a blind panel on the left side of the rectangular channel at (5.0 cm) from the test section entrance. The water pumped with maximum discharge of 500 l/min from the water tank and forced into the test section. Flow meter is used to measure volume flow rate of water with range (0-30 l/min). The air compressor with a specification capacity (0.5 m<sup>3</sup>) and maximum pressure (16 bar) is used to provide gas phase (air) into the test section. Air flow meter of range (5.833 l/min to 58.33 l/min), is used to measure and control the volume flow rate of air. The electrical voltage provided into the heaters by a power supply with a maximum voltage (220 V), with Digital Power Analyzer used to balance the electrical voltage across the heaters. Two Heater with total voltage is (220 V) supported into the channel at ribs side. A thermal camera was used to record the temperature distribution of the mixture (water and air) inside the channel, camera had a high accuracy of  $\pm 2^{\circ}\text{C}$  or  $\pm 2\%$ , with frame rate 9HZ. The air phase and the water phase are blended in a mixing device before they enter the channel.

Different values of water and air flow rates and constant heat flux were employed in order to measure the temperature in different working conditions. The values used are shown in Table (1).

**The present experimental procedures can be summarized as:**

- 1-The first rib (triangular shape) is attached inside the channel.
  - 2- Turn on water centrifugal pump at the initial value of (2 l/min).
  - 3- Supply the electrical power to the heaters at constant heat flux of (120 W).
  - 4- Wait few minutes (5-10 min) until the rib up to the desired temperature (42 C) by observing the temperature variations in different locations along the test section.
  - 5- Turn on the air compressor at the initial value of (8.33 l/min).
  - 6- Recording the temperature by sensors which are located at five points along the test section, and imaging the distribution of temperature by the thermal camera.
  - 7- The above steps are repeated for the four different values of air flow rate as given in Table (1).
  - 9- The above steps are repeated for the four different values of water flow rate as given in Table (1).
  - 10- All the above steps are repeated for the rectangular and semi-circle ribs.
- Superficial velocities were found for water and air and used in the graphs to show the effect of increasing it on the local heat transfer coefficient results and the temperature distribution. The flow rate was measured directly from the flow meter and used to calculate the superficial velocity according to Eq. (1) (Asano et al. 2004; Ansari and Arzandi. 2012).

$$U = \frac{Q}{A} \tag{1}$$

where

U = Liquid superficial velocity (m/s).

Q = Volume flow rate (m<sup>3</sup>/s).

A = Cross-sectional area (m<sup>2</sup>).

### NUMERICAL SIMULATION

Numerical simulation was performed for each experiment of test using Ansys Fluent 15.0. The model was assumed as two dimensional geometry structure modeled with Ansys Workbench 15.0. In this work, the geometry of the rectangular channel was divided elements (Quadrilateral structured grid) using the Meshing combined with Ansys Workbench 15.0 with maximum and minimum size equal to (0.002 m). The number of elements were (5188, 5200, 5277, and 5283) for rectangular ribbed, semi-circle ribbed, triangular ribbed, and smooth channel. The model governing equations would be solved at each element of the model geometry. Fig. (3) shows the mesh of the smooth and channel with three types of ribs.

### BOUNDARY CONDITIONS

Boundary conditions used for this model are:

#### Inlet Velocity

The bottom edge of the rectangular channel which represented inlet of the channel. The superficial velocities of water and air was used as the inlet boundary condition, which is set as

$$U_x = 0, U_y = \text{inlet velocity}, T_{in} = 287 \text{ K}$$

$$\frac{\partial}{\partial x}(U_x) = 0, \frac{\partial}{\partial x}(U_y) = 0$$

#### Wall

Left side wall of the smooth and ribbed rectangular channel at ribs was exposed to a constant heat flux (120 W). While the remaining portion of the channel wall was set to be adiabatic.

#### Outlet

The outlet of the channel was set as an outlet pressure.

The boundary conditions are presented in Table (2). Relaxation factors used for the numerical simulations in fluent model are shown in Table (3).

### GOVERNING EQUATIONS

Mixture model solves the conservation equations of continuity, momentum, and energy for each phase, a mixture model was used where the phases moved at different velocities. The governing equations can be written as (Fluent User’s Guide, 2006):

#### Continuity Equation

The general form of this equation is given by:

$$\frac{\partial}{\partial t}(\rho_m) + \nabla \cdot (\rho_m \vec{v}_m) = 0 \tag{2}$$

The mass-averaged velocity  $\vec{u}_m$  is represented as:

$$\vec{u}_m = \frac{\sum_{k=1}^n \alpha_k \rho_k \vec{u}_k}{\rho_m} \quad (3)$$

and  $\rho_m$  is the density of mixture :

$$\rho_m = \sum_{k=1}^n \alpha_k \rho_k \quad (4)$$

$\alpha_k$  is the volume fraction of phase  $k$ .

### Momentum Equation

The general form of this equation is given by:

$$\frac{\partial}{\partial t} (\rho_m \vec{u}_m) + \nabla \cdot (\rho_m \vec{u}_m \vec{u}_m) = -\nabla P + \nabla \cdot [\mu_m (\nabla \vec{u}_m + \nabla \vec{u}_m^T)] + \rho_m \vec{g} + \vec{F} + \nabla \cdot \left( \sum_{k=1}^n \alpha_k \rho_k \vec{u}_{dr,k} \vec{u}_{dr,k} \right) \quad (5)$$

Where  $n$  is the number of phases ,  $\vec{F}$  is a body force, and  $\mu_m$  is the viscosity of the mixture, which is given by:

$$\mu_m = \sum_{k=1}^n \alpha_k \mu_k \quad (6)$$

Where  $\vec{u}_{dr,k}$  is the drift velocity for secondary phase  $k$ :

and

$$\vec{u}_{dr,k} = \vec{u}_k - \vec{u}_m \quad (7)$$

### Energy Equation

The general form of this equation is given by:

$$\frac{\partial}{\partial t} \sum_{k=1}^n (\alpha_k \rho_k E_k) + \nabla \cdot \sum_{k=1}^n (\alpha_k \vec{u}_k (\rho_k E_k + P)) = \nabla \cdot (\mathbf{k}_{eff} \nabla T) + S_E \quad (8)$$

where  $\mathbf{k}_{eff}$  is the effective conductivity  $(\sum \alpha_k (\mathbf{k}_k + \mathbf{k}_t))$ , where  $\mathbf{k}_t$  is the turbulent thermal conductivity. The first term on the right-hand side of Eq. (8) represents energy transfer due to conduction.  $S_E$  includes any other volumetric heat sources.

### Turbulence Model

Ansys Fluent 15.0 displays three methods for k-ε turbulence model for the two-phase flow which are:

1. Turbulence mixture model
2. Turbulence dispersed model
3. Turbulence model for each phase

Depending on the deviation between experimental and numerical results, being choosing the turbulence  $k$  - $\varepsilon$  standard mixture model was set for the two phases model which can be defined through these equations (Fluent User's Guide, 2006 ).

$$\frac{\partial}{\partial t}(\rho_m k) + \nabla \cdot (\rho_m \vec{v}_m k) = \nabla \cdot \left( \frac{\mu_{t,m}}{\sigma_k} \nabla k \right) + G_{k,m} - \rho_m \varepsilon \quad (9)$$

$$\frac{\partial}{\partial t}(\rho_m \varepsilon) + \nabla \cdot (\rho_m \vec{v}_m \varepsilon) = \nabla \cdot \left( \frac{\mu_{t,m}}{\sigma_\varepsilon} \nabla \varepsilon \right) + \frac{\varepsilon}{k} (C_{1\varepsilon} G_{k,m} - C_{2\varepsilon} \rho_m \varepsilon) \quad (10)$$

where  $\varepsilon$  is the turbulent dissipation rate,  $G_k$  is the generation of turbulence kinetic energy, and  $\sigma$  is the turbulent Prandtl number for  $k$  and  $\varepsilon$ .

The density and the velocity of the mixture,  $\rho_m$  and  $\vec{v}_m$ , are computed as following:

$$\rho_m = \sum_{i=1}^n \alpha_i \rho_i \quad (11)$$

$$\vec{v}_m = \frac{\sum_{i=1}^n \alpha_i \rho_i \vec{v}_i}{\sum_{i=1}^n \alpha_i \rho_i} \quad (12)$$

The turbulent viscosity,  $\mu_{t,m}$ , and the production of turbulence kinetic energy,  $G_{k,m}$ , are computed as:

$$\mu_{t,m} = \rho_m C_\mu \frac{k^2}{\varepsilon} \quad (13)$$

$$G_{k,m} = \mu_{t,m} \left( \nabla \cdot \vec{v}_m + (\nabla \cdot \vec{v}_m)^T \right) : \nabla \vec{v}_m \quad (14)$$

The model constants are given in Table (4).

## 6. HEAT TRANSFER COEFFICIENT

The rate of heat transfer is the amount of heat that is transferred per unit time (usually per second). The local heat transfer coefficient by convection between the surface of the heated plate (rib) and mixture of two phase flow can be written as (Wang et al. 2010; Lim et al. 2013; Fluent User's Guide. 2006):-

$$h_x = \frac{q}{A_r (T_s - T_f)} \quad (15)$$

where  $q$  is the heat flux (W), and is regularly distributed over the test section,  $A_r$  is the surface area of the rib,  $T_s$  is the surface temperature of the rib which is measured by thermocouple, and  $T_f$  is the local fluid temperature.

## 7. UNCERTAINTY ANALYSIS

All the quantities (heat flux and temperature) that are measured to estimate the local heat transfer coefficient are subject to certain uncertainties due to errors in the measurement. These individual uncertainties as well as the combined effect of these are presented here. The error may result either from the experimental or from the instrument or both. So, the analysis of error for any experimental is required to be determined.

The experimental result  $R$  is a given function of the independent variables  $x_1, x_2, x_3, \dots, x_n$ , thus:  
 $R=R(x_1, x_2, x_3, \dots, x_n)$  (16)

If we define  $W_R$  as the uncertainty in the results, and  $w_1, w_2, \dots, w_n$  denote to the uncertainty in the independent variables, then the uncertainty in the results can be written as:

$$w_R = \left[ \left( \frac{\partial R}{\partial x_1} \times w_1 \right)^2 + \left( \frac{\partial R}{\partial x_2} \times w_2 \right)^2 + \dots + \left( \frac{\partial R}{\partial x_n} \times w_n \right)^2 \right]^{0.5}$$
 (17)

Equation (17) can be used to estimate the uncertainty in each of local heat transfer coefficient.

For our experiment of heat transfer enhancement of two-phase flow in a vertical rectangular channel using different ribs, case1 (triangular rib) is taken as an example. The following input data of the input voltage (V) and the current (I) are as follows:

$$V=107 \text{ volt} \quad , \quad I= 1.5 \text{ A}$$

The uncertainty in the total convection heat transfer rate from the heated plate (rib) can be calculated as follows:

$$q = \text{Power input} = I \times V$$
 (18)

$$I= 1.5A \pm 0.02 \text{ A} \quad , \quad V= 107 \text{ v} \pm 0.03 \text{ v}$$

$$W_I = 0.02 \text{ A} \quad , \quad W_V = 0.03 \text{ v (AL-Taee and Jurmut. 2014)}$$

$$\text{Thus } q = 160.5 \text{ W}$$

$$\frac{\partial q}{\partial I} = V = 107 \text{ v} \quad \text{and} \quad \frac{\partial q}{\partial V} = 1.5 \text{ A}$$

$$w_q = \left[ \left( \frac{\partial q}{\partial I} \times w_I \right)^2 + \left( \frac{\partial q}{\partial V} \times w_V \right)^2 \right]^{0.5}$$
 (19)

$$w_q = 0.0214$$

The uncertainty of local heat transfer coefficient for the channel with ribs can be calculated as follows:

$$h_x = \frac{q}{A_r (T_s - T_f)}$$
 (20)

$$wh_x = \left[ \left( \frac{\partial h_x}{\partial q} \times wq \right)^2 + \left( \frac{\partial h_x}{\partial A_r} \times wA_r \right)^2 + \left( \frac{\partial h_x}{\partial T_s} \times wT_s \right)^2 + \left( \frac{\partial h_x}{\partial T_f} \times wT_f \right)^2 \right]^{0.5} \quad (21)$$

Assume uncertainty of the surface area of rib ( $wA_r$ ) = 0, and uncertainty of surface rib and local fluid temperatures ( $wT_s$ ,  $wT_f$ ) = 0.09 (from calibrated data in Appendix A).

Table (5) give a detailed calculation of the uncertainty of local heat transfer coefficient.

## RESULTS AND DISCUSSIONS

The experimental and numerical heat transfer coefficient results were drawn together in order to compare between them, where solid and dotted lines represented the experimental and numerical results, respectively. Furthermore, the distribution of temperature along the channel was photographed using thermal camera and compared with images for the corresponding contours which found numerically. The numerical results seemed to have the same influence as the experimental results with a deviation of about (6.0 %) found between them. This is because, it was a changed phenomenon and controlled by different parameters that being assumed throughout these simulations, so those values can be changed by making different assumptions. Two phase (water-air) flow through rectangular channel that roughed with different shapes ribs (rectangular, semi-circle, and triangular) was investigated using ANSYS Fluent 15.0. Five values of water and air velocities was studies. Figure (4) shows the local heat transfer coefficient for the three shapes of ribs with respect to the air superficial velocity and at different values of the water superficial velocity and heat flux. When water superficial velocity increase, the heat transfer coefficient increase due to the decrease in the time residence of mixture (water and air) and increase the amount of water inside the channel, and adding of ribs increase surface area of heat transfer and interrupt the development of boundary layer of flow and create turbulence flow inside the channel. Thus the triangular rib had a higher rate of heat transfer of the other ribs, because it had a sharp edge and smallest tip, so the area for the leading edge and the trailing edge behavior was at its biggest value for the rectangular ribs and at its smallest value for the triangle ribs and this provides additional area for heat transfer and generated a turbulence flow higher than the other ribs (semi- circle and rectangular). In addition, it can be said that more increase in the heat transfer augmentation for triangular and semi-circle ribbed channel is due to the fact that the flow mixing and sweeping surface in these types of ribs are more than those of the rectangular ribs. One can conclude that the flow mixing and disturbances for the triangular rib were more than that for the other ribs. Figures (5) to (7), demonstrate the contours of temperature distribution for the three ribbed channels experimentally and numerically. Each figure is for five values of water superficial velocity with a constant value of air superficial velocity and heat flux. These figures show that the amplitude appeared at a certain location which where the ribs located. Figure (5) show the effect of water superficial velocity on the contours of temperature distribution inside the channel ribbed with triangular shape at constant values of air superficial velocity and heat flux. As the superficial velocity of water increased the temperature distribution decreased inside the channel. The reason for this effect was a result of increasing the superficial velocity of water and decreases the time residence of mixture inside the channel which caused an increase in the water flow rate and reduced the temperature difference along the channel. Figure (6) offer the contours of temperature distribution through channel supplied with semi-circle rib at constant values of air superficial velocity and heat flux. The

temperature distribution over the walls of the ribs decreased as the water superficial velocity increased due to the increase in the amount of water and decreases the time residence of mixture inside the channel. Figure (7) display the contours of temperature distribution through channel fitted with rectangular rib at constant values of air superficial velocity and heat flux. As the water superficial velocity increased, the distributions of the temperature decreased due to the increase in the amount of water and decrease the time residence of mixture inside the channel.

## COMPARISON BETWEEN SMOOTH AND RIBBED CHANNEL

Heat transfer was investigated for both smooth and ribbed channels. The investigation was performed experimentally and numerically and the results of smooth channel were compared with the ribbed one, for the same boundary conditions. Figure (8) shows the heat transfer coefficient for both smooth and ribbed channel at different superficial velocities of water and air and constant heat flux (120 W). It can be shown that the heat transfer coefficient for channel fitted with three shape of ribs (triangular, semi-circle, and rectangular) was greater that smooth channel by (75% for channel fitted with triangular rib), by (59% for channel fitted with semi-circle rib), and by (45% for channel fitted with rectangular rib). The percentage increase in the heat transfer coefficient was calculated using equation (22).

$$\text{Percentage increase} = \frac{h_{\text{smooth}} - h_{\text{ribbed}}}{h_{\text{smooth}}} \quad (22)$$

Attributing the cause of this effect to the presence of the ribs in the channels, where these ribs provides additional surface area for heat transfer and creates a turbulence flow by breaking the laminar-sub layer, and as a result of this effect, the heat transfer coefficient results increase because of both increasing surface area and increasing turbulence. Thus the triangular rib had a higher rate of heat transfer of the other ribs, because it had a sharp edge and smallest tip, so the area for the leading edge and the trailing edge behavior was at its biggest value for the rectangular ribs and at its smallest value for the triangle ribs and this provides additional area for heat transfer and generated a turbulence flow higher than the other ribs (semi- circle and rectangular).

## CONCLUSIONS

In this paper the two phase heat transfer coefficient for ribbed and smooth channel was investigated experimentally and numerically using Ansys Fluent 15.0 software. The heat transfer coefficient of the ribbed channel was compared with the smooth channel and found to be increased by 45 % for rectangular ribbed channel, 59 % for semi-circle ribbed channel, and 75 % for triangular ribbed channel, so, the triangular rib is the best shape to enhance the rate of heat transfer, whereas the rectangular rib is the worst one to enhance it. It also found that the heat transfer coefficient increase as the velocity of the flow increase. The temperature distribution was shown to be formed at the trailing edge of the ribs and the temperature found to be at its higher value at the trailing edge of the ribs and for the three types of ribs.

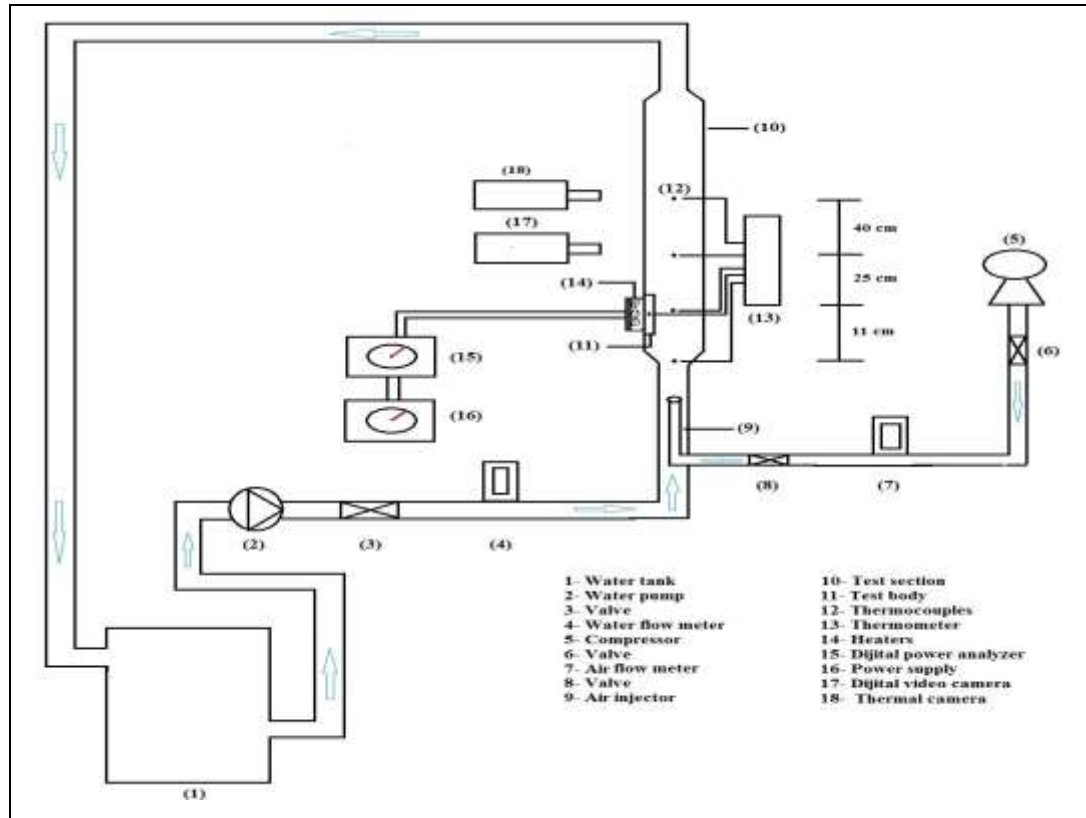


Figure (1) :The Experiment Schematic Diagram

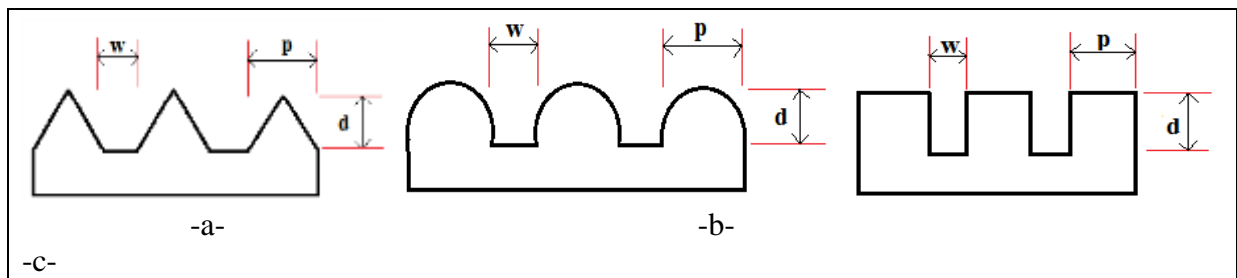


Figure (2): Ribs Shape

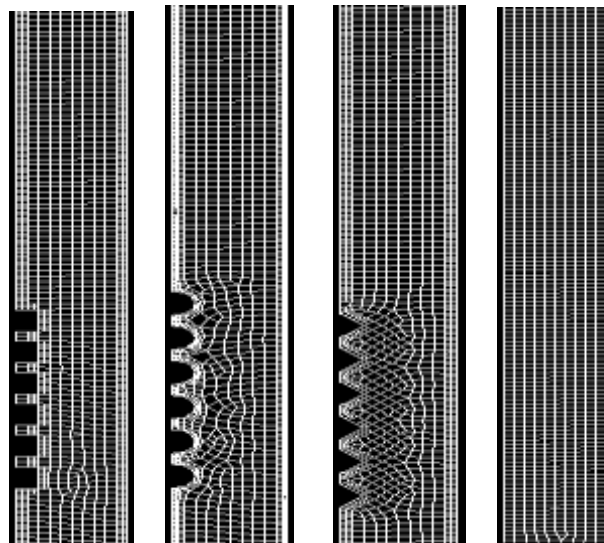
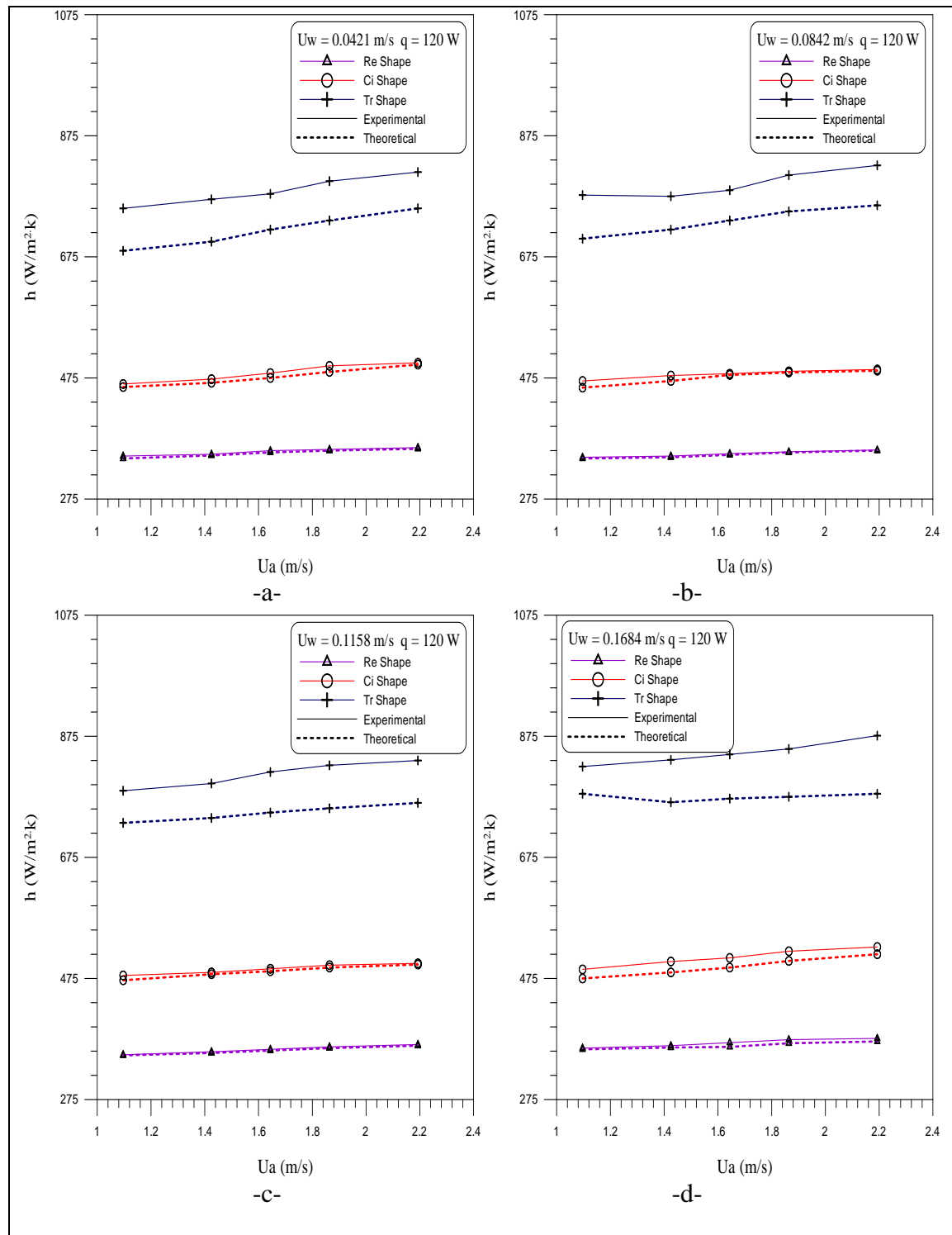
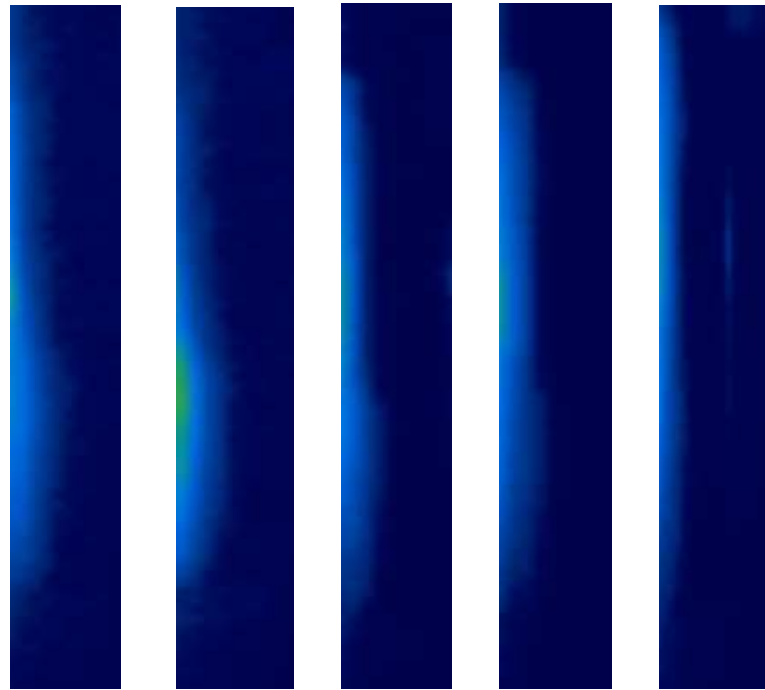


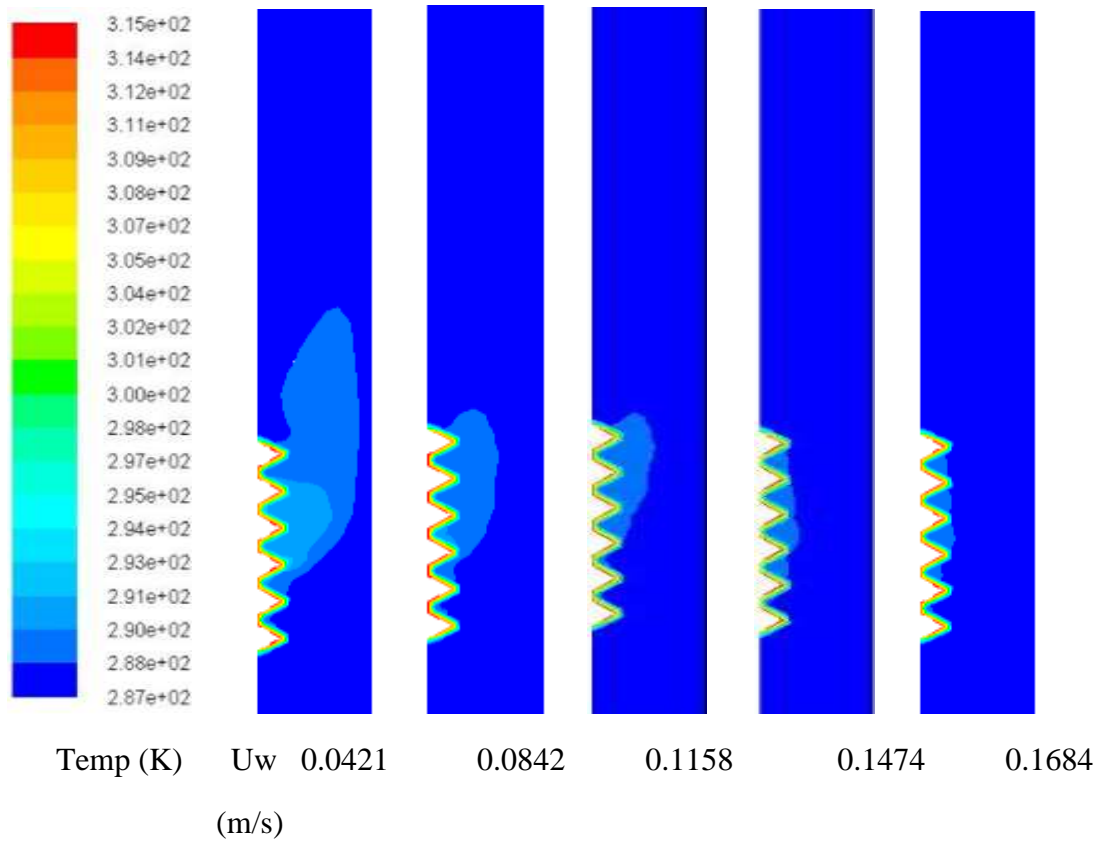
Figure (3): The Mesh of Smooth and Ribbed Channel



**Figure (4):** Effect of Rib Shape on the Heat Transfer Coefficient at Constant Water Superficial Velocity and Heat Flux

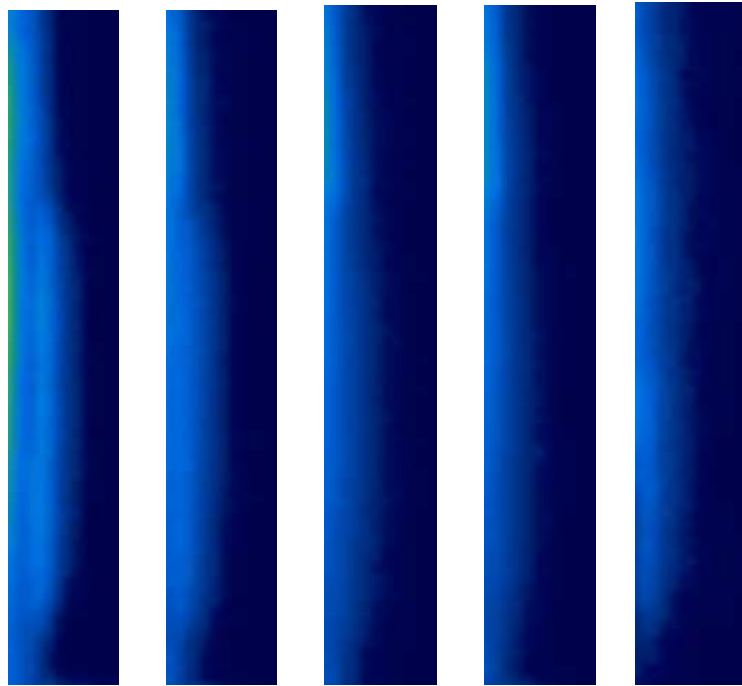


a. Experimental

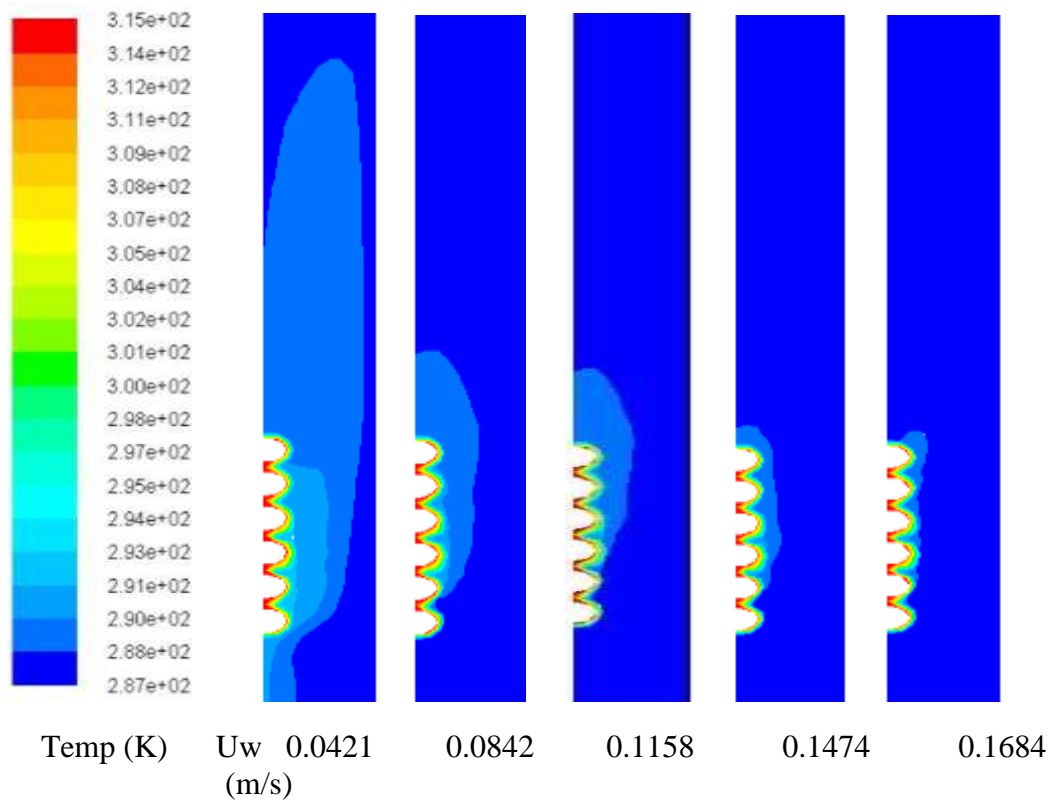


b. Numerical

**Figure (5):** Effect of Water Superficial Velocity on Temperature Distribution at 1.0964 m/s Air Superficial Velocity and Heat Flux (120 W) for Triangular Rib

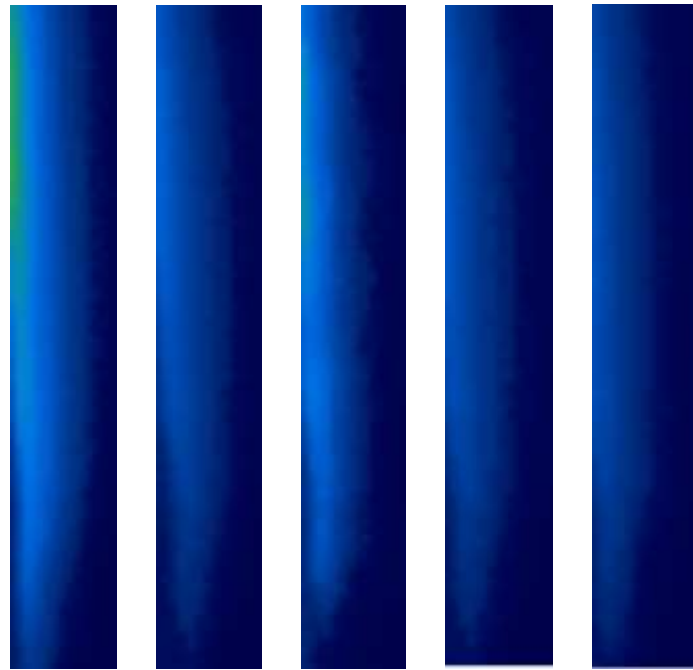


a. Experimental

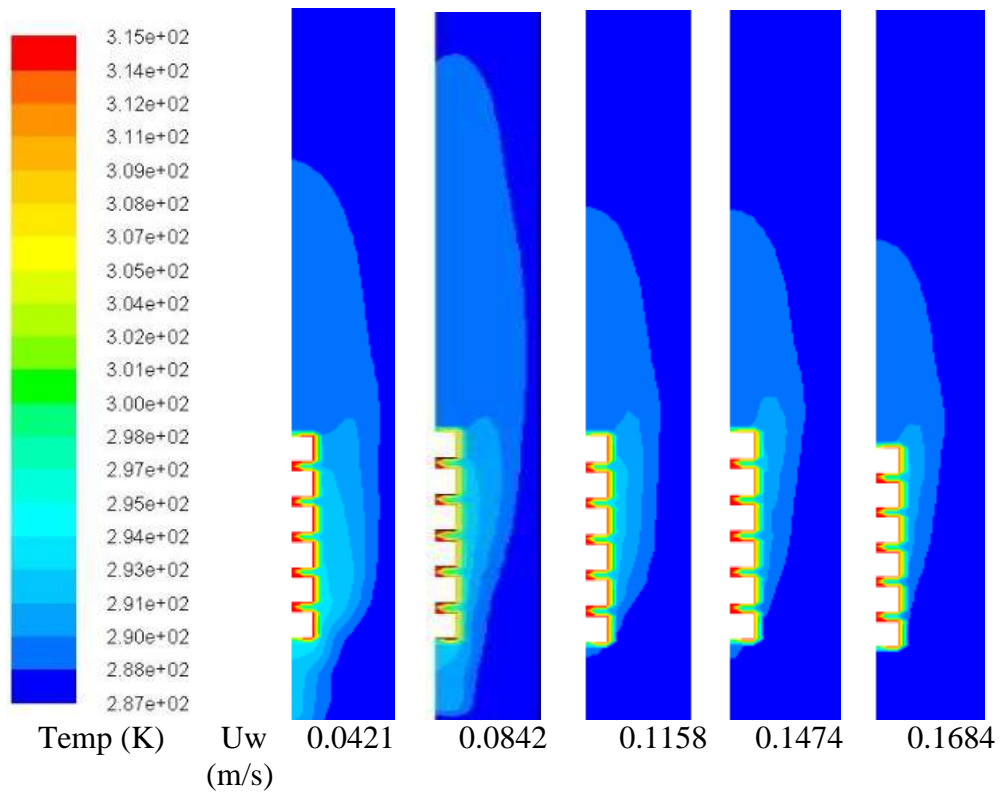


b. Numerical

**Figure (6):** Effect of Water Superficial Velocity on Temperature Distribution at 1.0964 m/s Air Superficial Velocity and Heat Flux (120 W) for Semi-Circle Rib



a. Experimental



b. Numerical

**Figure (7):** Effect of Water Superficial Velocity on Temperature Distribution at 1.0964 m/s Air Superficial Velocity and Heat Flux (120 W) for Rectangular Rib

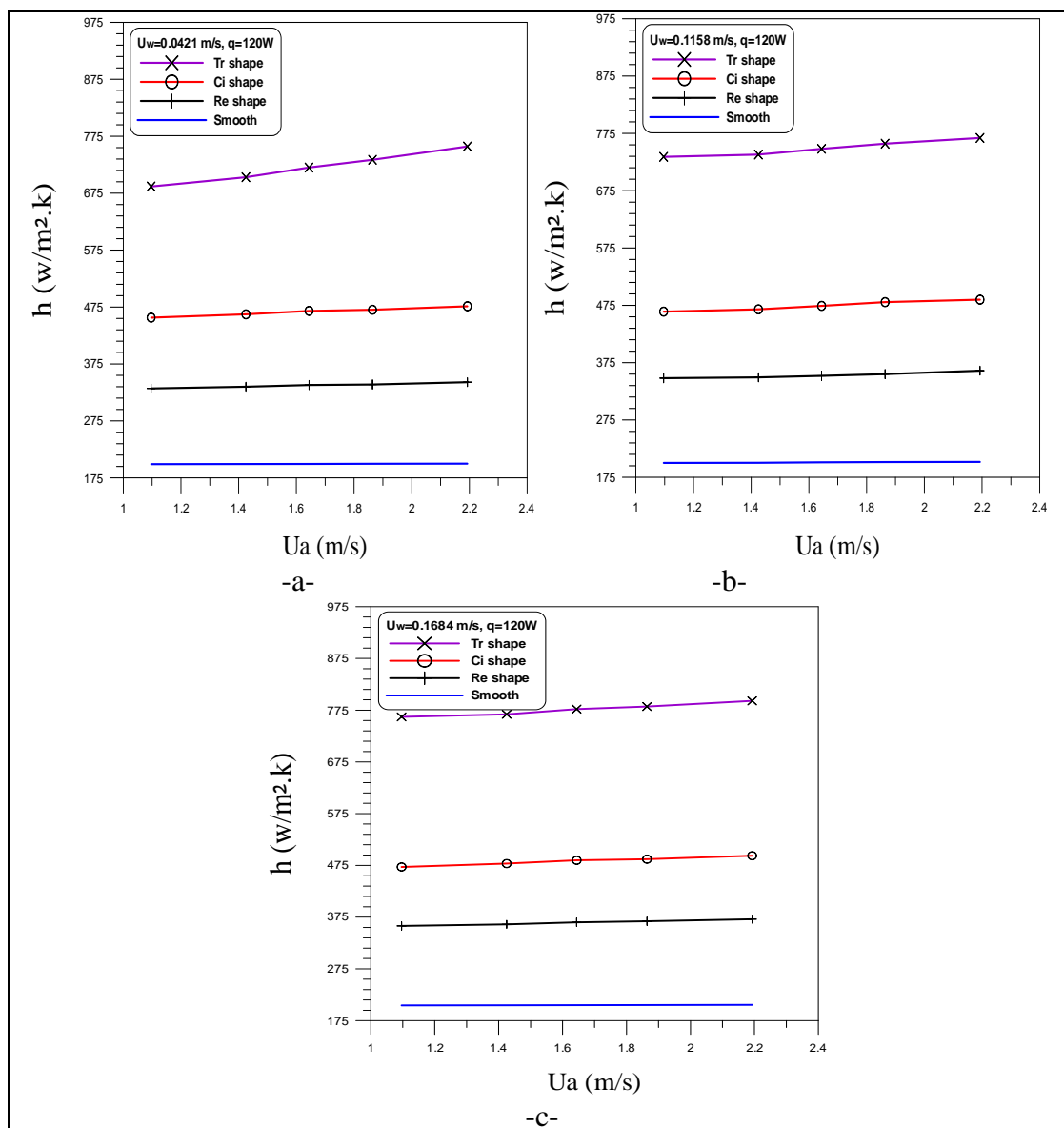


**Figure (8):** Comparison the Local Heat Transfer Coefficient of Smooth and Ribbed Channel at Constant Heat Flux 120W

**Table (1):** Values of work conditions used in experiments

Heat flux $q$ (W)	Water discharge (l/min)	Air discharge (l/min)
120	2	8.33
-	4	10.83
-	5.5	12.5
-	7	14.167
-	8	16.67

**Table (2):** Zones Boundary Conditions

Zone	Boundary Type
	Two phases (Water-Air)
Channel inlet W	Water superficial velocity
Channel inlet A	Air superficial velocity
Channel outlet	Outlet pressure
Channel side	Heat flux
Channel content	Water – Air

**Table (3):** Model Relaxation

Variable	Relaxation factors
	Two phases (Water-Air)
Pressure	0.3
Momentum	0.5
Volume fraction	0.5
Energy	0.8

**Table (4):** Model Constants

The constant	Value
$\sigma_k$	1.00
$\sigma_\varepsilon$	1.30
$C_{1\varepsilon}$	1.44
$C_{1\varepsilon}$	1.92
$C_\mu$	0.09

**Table (5):** Local Heat Transfer Coefficient Uncertainty

Water flow rate (l/min)	Air flow rate (l/min)	Uncertainty hx
2	8.33	0.0278
4	10.83	0.0305
5.5	12.5	0.0337
7	14.167	0.0361
8	16.67	0.0386

## REFERENCES

Al-Turaihi, R. S., and Oleiwi, S. H., “Heat Transfer of Two Phases (Water–Air) in Horizontal Smooth and Ribbed Ducts”, *International Journal of Energy Applications and Technologies*, V. 3, No. 2, 41-49, 2016.

Ansari, M. R. and Arzandi, B., “Two-phase gas–liquid flow regimes for smooth and ribbed rectangular ducts”, *International Journal of Multiphase Flow*, PP. 118-125, 2012.

Asano, H., Takenaka, N., and Fujii, T., “Flow characteristics of gas–liquid two-phase flow in plate heat exchanger (Visualization and void fraction measurement by neutron radiography)”, *Experimental Thermal and Fluid Science*, Japan, V. 28, No. 2, PP. 223–230, 2004.

Habeeb, L. J. , and Al-Turaihi, R. S. ,“ Experimental Study and CFD Simulation of Two-Phase Flow around Multi-Shape Obstacles in Enlarging Channel”, *American Journal of Mechanical Engineering*, Vol. 1, No. 8, PP. 470-486, 2013.

Jalghaf, H. K. , Al-Turaihi, R. S., and Habeeb, L. J., “Air-Water Flow Investigation around Hot Circular Cylinder inside Channel”, *Advances in Natural and Applied Sciences*, V. 10, No. 12, PP. 16-27, 2016.

Jayakumar, J. S., Mahajani, S. M., Mandal, J. C., Iyer, K. N., and Vijayan, P. K, “Thermal hydraulic characteristics of air–water two-phaseflows in helical pipes”, *chemical engineering research and design*, V.88, No. 4, PP. 501–512, 2010.

Manca, O., Nardini S., and Ricci D., “Numerical Study of Air Forced Convection in a Chanel Provided with Inclined Ribs”, *Frontiers in Heat and Mass Transfer (FHMT)*, 2011.

Saha, S., and Saha, S. K. ,“Enhancement of heat transfer of laminar flow through a circular tube having integral helical rib roughness and fitted with wavy strip inserts”, *Experimental Thermal and Fluid Science*, V. 50, PP. 107-113, 2013.

Shedd, T. A., and Newell, T. A., “Visualization of two-phase flow through microgrooved tubes for understanding enhanced heat transfer”, *International Journal of Heat and Mass Transfer*, V. 46, No.22, PP. 4169–4177, 2003.

Vlasogiannis, P., Karagiannis, G., Argyropoulos, P., and Bontozoglou, V., “Air–water two-phase flow and heat transfer in a plate heat exchanger”, *International Journal of Multiphase Flow*, V. 28, No. 5, PP. 757-772, 2002.

Wang, X., Wang, W., Chou, L., Han, Y., Xu, L., and Shui, “Flow and Heat Transfer of Air and Steam in Internal Cooling Passages of Turbine”, *American Society of Mechanical Engineers, Power for Landa: Power for Land, Sea, and Air*, PP.1-10, 2010.